Title

Impacts of Forest Fire Ash on Aquatic Mercury Cycling

Journal

Environmental Science and Technology, 56(16)

ISSN

0013-936X

Authors

Li, Han-Han
Tsui, Martin Tsz-Ki
Ku, Peijia
et al.

Publication Date

2022-08-16

DOI

10.1021/acs.est.2c01591

Peer reviewed

Environmental Science & Technology

pubs.acs.org/est

Article

Impacts of Forest Fire Ash on Aquatic Mercury Cycling

Han-Han Li, Martin Tsz-Ki Tsui,* Peijia Ku, Huan Chen, Ziyu Yin, Randy A. Dahlgren, Sanjai J. Parikh, Jianjun Wei, Tham C. Hoang, Alex T. Chow, Zhang Cheng,* and Xue-Mei Zhu*

Cite This: *Environ. Sci. Technol.* 2022, 56, 11835−11844

Read Online

ACCESS | Metrics & More | Article Recommendations | Supporting Information

ABSTRACT: Mercury (Hg) is a ubiquitous contaminant in the environment and its methylated form, methylmercury (MeHg), poses a worldwide health concern for humans and wildlife, primarily through fish consumption. Global production of forest fire ash, derived from wildfires and prescribed burns, is rapidly increasing due to a warming climate, but their interactions with aqueous and sedimentary Hg are poorly understood. Herein, we compared the differences of wildfire ash with activated carbon and biochar on the sorption of aqueous inorganic Hg and sedimentary Hg methylation. Sorption of aqueous inorganic Hg was greatest for wildfire ash materials (up to 0.21 μg g^{-1} or 2.2 μg g^{-1} C) among all of the solid sorbents evaluated. A similar Hg adsorption mechanism for activated carbon, biochar made of walnut, and wildfire ash was found that involves the formation of complexes between Hg and oxygen-containing functional groups, especially the −COO group. Notably, increasing dissolved organic matter from 2.4 to 70 mg C L^{-1} remarkably reduced Hg sorption (up to 40% reduction) and increased the time required to reach Hg−sorbent pseudo-equilibrium. Surprisingly, biochar and wildfire ash, but not activated carbon, stimulated MeHg production during anoxic sediment incubation, possibly due to the release of labile organic matter. Overall, our study indicates that while wildfire ash can sequester aqueous Hg, the leaching of its labile organic matter may promote production of toxic MeHg in anoxic sediments, which has an important implication for potential MeHg contamination in downstream aquatic ecosystems after wildfires.

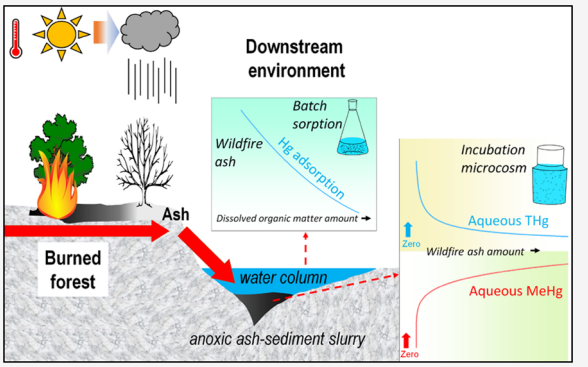

KEYWORDS: *wildfire ash, activated carbon, biochar, aqueous mercury sorption, mercury methylation*

INTRODUCTION

Forest fires, including both wildfire and prescribed fires, are important drivers of biogeochemical alterations to forest ecosystems.[1] The frequency and intensity of wildfires are rapidly increasing, partly attributable to global climate change,[2] while prescribed fire is also becoming more prevalent as a forest management tool.[3] Further, these fires of various intensities and durations have produced various effects on the biogeochemical cycles of downstream aquatic systems, such as carbon and nitrogen cycling.[4]

Mercury (Hg) is a pollutant of global concern as it contaminates all geographical areas owing to its widespread emissions (e.g., both natural and anthropogenic), long-range atmospheric transport, and dry/wet deposition.[5] Forest ecosystems are an important sink of Hg due to enhanced sequestration via foliar uptake[6] and can also become a source of Hg during/after forest fires via volatilization (for atmospheric transport) and runoff/erosion (to aquatic ecosystems).[7] While much of the Hg in biomass has been shown to be volatilized during forest fires,[8] the remaining ash may still contain significant amounts of Hg derived from the burned vegetation.[9] For example, total Hg concentrations up to 125 ng g^{-1} dry wt were measured in ash after a northern California wildfire, which would be even higher than litter (up to 40 ng g^{-1}) and dead woody materials collected in a nearby site (up to 57 ng g^{-1}).[9]

In aquatic sediments, the methylation of inorganic Hg [Hg(II)] by anaerobic bacteria produces highly toxic methylmercury [MeHg].[10] Mercury methylation is a key step for Hg to enter the base of aquatic food webs, and subsequently MeHg biomagnifies along the food chain, leading to unsafe levels for the top aquatic predators.[11] Recently, Ku et al.[9] demonstrated that wildfire ash materials are capable of effectively sequestering Hg(II) from natural waters and evaluated the interactive behavior of ash and Hg with respect to a few ash properties [e.g., percent loss-on-ignition (LOI) and aromatic hydrocarbon (ArH) fraction], raising an important but largely unanswered question: How might forest fire ash interact with aqueous Hg(II) and mediate sedimentary Hg methylation after fire events?

Received: March 5, 2022
Revised: June 21, 2022
Accepted: July 20, 2022
Published: July 29, 2022

Interactions of Hg with wildfire ash provide an interesting comparison to the numerous studies in the last few decades examining the effectiveness of activated carbon and biochars on the removal of aqueous Hg(II) and inhibition of Hg methylation in sediments. For example, an early study demonstrated the efficient removal of Hg(II) by activated carbon.[12] Recently, Gilmour et al.[13] showed the effectiveness of activated carbon in mitigating MeHg formation in Hg-contaminated sediments, while Gilmour et al.[14] successfully applied activated carbon in remediation of a Hg-contaminated saltmarsh. Similarly, the use of biochar has been widely evaluated, mostly in the laboratory, for removing aqueous Hg[15−19] and reducing Hg methylation in sediment/soil and subsequent MeHg bioaccumulation.[20,21]

While the precise mechanism of Hg(II) sorption by wildfire ash is currently unknown,[9] previous studies have posited a similar mechanism for Hg sorption for both activated carbon and biochar, specifically the formation of $(COO)_2Hg$ and $(O)_2Hg$ complexes.[19] However, a myriad of environmental factors may compromise the effectiveness of these sorbents for Hg removal, such as dissolved organic matter (DOM). DOM has been recently shown to reduce the effectiveness of activated carbon and biochar in sequestering aqueous Hg(II), presumably through formation of aqueous Hg-DOM complexes via the thiol group.[22,23] It may be worth noting that no study of Hg sequestration by wildfire ash has evaluated the impact of different DOM concentrations and that DOM has consistently been documented to increase in aquatic systems post-wildfire.[24] Thus, complex biogeochemical interactions must be considered when evaluating how solid-phase sorbents (e.g., wildfire ash) interact with Hg in natural aquatic environments (e.g., different DOM levels).

Due to the increasing extent of global wildfires[2,25] and the use of prescribed burning for forest management,[3] there is an urgent need to better understand how these solid-phase sorbents mediate Hg cycling in downstream aquatic environments, especially in a range of DOM levels. In this work, we compared the effectiveness of two wildfire ash, four laboratory-controlled burn ash, one commercial activated carbon, and two biochar samples for aqueous Hg removal and sedimentary Hg methylation. Our findings demonstrated strong sequestration of aqueous Hg(II) by all solid sorbents, but there is potential for the forest fire ash materials to stimulate microbial Hg(II) methylation when incubated in anoxic sediments.

MATERIALS AND METHODS

Solid Sorbent Materials. In this study, we used two wildfire ash samples (sieved < 2 mm) produced by low-severity wildfires, i.e., wildfire ash 1 (Wragg Fire, July 22−August 5, 2015, no rainfall prior to sampling) and wildfire ash 2 (Rocky Fire, July 29−August 14, 2015, no rainfall prior to sampling), in northern California, more details of wildfire site characteristics and sampling information can be found in Table S1 and Text S1. In a subset of experiments, we used ash samples generated by laboratory-controlled burning (i.e., 250*ox*, 250*py*, 550*ox*, 550*py*) in a laboratory under different temperatures (i.e., 250 and 550 °C) and the presence/absence of oxygen [i.e., pyrolysis (py) vs thermal oxidation (ox)] from white fir (Abies concolor) litter.[26] For comparison, we included a commercially available activated carbon (−20 + 40 mesh, CAS 7440-44-0, Alfa Aesar, Lancashire, UK) that was also used in our previous study.[9] The size of activated carbon particles ranged from 0.8 to 2.4 mm, which would be comparable to the size of our sieved ash samples. Further, we assessed two biochar samples ($biochar_{walnut}$—walnut shell/gasification and $biochar_{sawdust}$—sawdust/hydropyrolysis)[27] with similar carbon content (i.e., ∼63% C), but very different Hg sorption capacities based on our preliminary tests. All solid sorbents were stored dry in the laboratory prior to use and analyzed for total Hg [THg] to assess their native Hg content (see Analytical Measurements section).

Aqueous Sorption. We evaluated the capability of the solid sorbents to remove aqueous Hg(II) in which we performed three experiments to examine the equilibrium adsorption: the effects of initial Hg(II) levels (0.5−10 $\mu g\ L^{-1}$), contact time (0.5−48 h), and different dissolved organic carbon (DOC) sources/levels (low-, mid-, and high-DOC at 2.4, 33.4, and 69.5 mg C L^{-1}, respectively) on aqueous Hg(II) sorption. Stock solutions with different DOC levels (i.e., "low-DOC", "mid-DOC", and "high-DOC") were generated in the laboratory and/or collected from the field. Briefly, low-DOC water was prepared as a synthetic freshwater in the laboratory (i.e., moderately hard water).[28] Mid-DOC water was collected from a freshwater wetland located in eastern North Carolina. High-DOC water was produced by incubating natural leaf litter of mixed deciduous species in the laboratory with low-DOC water for 2 days. We filtered all three water types through a 0.7 μm filter (Whatman GF/F) prior to use. For all sorption experiments, we prepared a stock solution of Hg(II) at 1 $\mu g\ mL^{-1}$ from reagent-grade $HgCl_2$ powder (Alfa Aesar) in laboratory-purified water (Barnstead Nanopure; 18.2 $M\Omega \cdot cm^{-1}$) and stored at 4 °C in the dark until use. Working solutions with different Hg(II) concentrations were prepared by diluting the stock solution with low-DOC, mid-DOC, and high-DOC waters.

Prior to sorption tests, we assessed the interactions of Hg and DOC between the solid sorbents and three DOC water types. Specifically, 0.50 ± 0.05 g of each solid sorbent (note: laboratory-controlled burn ash was not used in all tests due to limited availability) was added to 100 mL of each DOC water type in a 500 mL Erlenmeyer glass flask (performed in triplicate) in which the ratio of sorbent mass to water volume (i.e., 0.5%) would be comparable to another recent Hg sorption study (e.g., 0.3%).[22] The initial pH of the test solution was adjusted to 7.80 ± 0.10 with a benchtop pH meter (Mettler Toledo), which would be similar to streamwater in burned sites in northern California[24] and this pH value would be similar to another Hg sorption study.[22] All flasks were continuously agitated on an orbital shaker at a rate of 200 rpm at room temperature in the dark. After 48 h, the supernatant was filtered through a 1.0 μm filter (Whatman GF/B), and the filtrate was quantified for THg and DOC (see below).

First, we examined Hg(II) sorption to all solid sorbents with an initial Hg(II) concentration of 1 $\mu g\ L^{-1}$, which would be comparable to other aqueous Hg sorption studies (e.g., 2 $\mu g\ L^{-1}$)[22] but much lower than earlier Hg sorption studies (e.g., 2−20 mg L^{-1}).[12] Similar to the above conditions, we added 0.50 ± 0.05 g of each solid sorbent into 100 mL of different DOC water types. The sorption test lasted for 48 h with continuous agitation in the dark at room temperature, while the initial pH was adjusted to 7.80 ± 0.10. Control experiments without sorbents were included to account for the error generated by the Hg(II) adsorption on the inner surface of flasks. Equilibrium adsorption (q_e) of Hg was calculated as

https://doi.org/10.1021/acs.est.2c01591
Environ. Sci. Technol. 2022, 56, 11835−11844

$$q_e = [(C_0 - C_e) \times V]/(m) \quad (1)$$

where q_e (μg g^{-1}) is the quantity of adsorbed Hg per unit mass of sorbent, C_0 and C_e (μg L^{-1}) are the initial and equilibrium Hg concentrations, respectively; V (L) is the solution volume; and m is the dry mass of the solid sorbent in grams.

Since the carbon/organic carbon of the solid sorbent plays an important role in Hg(II) adsorption process,[19] thus, the equilibrium quantity (q_{ec}) of adsorbed Hg per unit mass of C for each sorbent was also calculated as

$$q_{ec} = [(C_0 - C_e) \times V]/(m \times C) \quad (2)$$

where q_{ec} (μg g^{-1} C) is the quantity of adsorbed Hg per unit mass of C; C_0 and C_e (μg L^{-1}) are the initial and equilibrium Hg concentrations, respectively; V (L) is the solution volume; m is the dry mass of the solid sorbent in grams; and C is the fraction of carbon of each solid sorbent.

Second, we evaluated the effect of initial Hg(II) concentration (C_0) using an adsorption isotherm approach with a range of C_0 (0.5−10 μg L^{-1}) for each solid sorbent (except laboratory-controlled burn ash), with the conditions as described above. The adsorption capacity and equilibrium constant were assessed by the Langmuir isotherm adsorption model as

$$q_e = (q_m \times K_L \times C_e)/(1 + K_L \times C_e) \quad (3)$$

where q_m (μg g^{-1}) is the maximum amount of adsorbed Hg per unit mass of sorbent and K_L (L μg^{-1}) is the constant for the Langmuir isotherm adsorption model.

Third, we investigated the effect of contact time on the sorption of Hg(II) by the solid sorbents in the three DOC water types (except laboratory-controlled burn ash). All conditions were the same as above except that a 10 mL aliquot was taken from the supernatant at selected time intervals (0.5, 1, 4, 8, 12, 24, 48 h) to determine the remaining aqueous Hg(II) concentrations.[29] Kinetic data were evaluated using pseudo-first-order (eq 4) and pseudo-second-order (eq 5) formulations

$$q_t = q_e(1 - e^{-k_1 t}) \quad (4)$$

$$q_t = (k_2 \times q_e^{\,2} \times t)/(1 + k_2 \times q_e \times t) \quad (5)$$

where q_t (μg g^{-1}) is the amount of adsorbed Hg(II) per unit mass of sorbent at time t, and k_1 (h^{-1}) and k_2 (g μg^{-1} h^{-1}) are the rate constants of the pseudo-first-order and pseudo-second-order models, respectively.

Sediment Incubation. Sediment incubation experiments were used to assess how the solid-phase sorbents affected both aqueous and sedimentary Hg(II) concentrations and mediated production of MeHg during anoxic incubation over 2 weeks. The experimental design was similar to our previous studies incubating litter only[30,31] and wildfire ash only.[9] However, we included a Hg-contaminated sediment (THg: 13.4 ± 0.8 μg g^{-1} dry wt.; MeHg: 3.5 ± 0.3 ng g^{-1} dry wt.) collected from the historically contaminated South River (Virginia)[32] in our incubation experiment to demonstrate whether wildfire ash would reduce sedimentary Hg(II) methylation effectively as demonstrated for activated carbon in other studies.[13]

We conducted the incubation experiments using South River water with each solid sorbent at concentrations of 1, 5, and 10% as dry mass of the sediment, but we only included the 5% treatment for the laboratory-controlled burn ash due to limited availability. Briefly, we placed both river water and sediment (control without solid sorbent or mixed with different solid-phase sorbent concentrations) (at a ratio of 10:1 v/w) into a 250 mL air-tight, sterile, Hg-free Nalgene poly(ethylene terephthalate) glycol (PETG) bottle (similar to our previous incubation experiments).[9,30,31] Triplicate bottles were included for all treatments. Bottles were tightly capped and placed in the dark at room temperature (~22 °C) for 2 weeks. The bottles were thoroughly shaken every day to mix the slurry. Aqueous samples were collected and passed through 1.0 μm Whatman GF/B filter at the end of the 2-week incubation to measure filtered THg, filtered MeHg, and DOC. To understand inorganic Hg and MeHg partitioning between solid and aqueous phases, post-incubation sediment samples from 5% sorbent addition treatments were collected and freeze-dried for subsequent THg and MeHg determination.

Spectroscopic Characterization. To gain further insight into Hg sorption mechanisms, the morphology and microstructure of three solid sorbents, namely, activated carbon, biochar$_{walnut}$, and wildfire ash 1, were examined using a field-emission scanning electron microscope (SEM, ZEISS Sigma). Samples were prepared by mounting biosorbent materials onto a conductive carbon tape and gently depositing nonadhesive silver powder via a N_2 flow. Samples were imaged at an accelerating voltage of 5 eV. X-ray photoelectron spectroscopy (XPS) was conducted to determine the surface chemical composition of activated carbon, biochar$_{walnut}$, and wildfire ash 1 before and after sorption of aqueous Hg(II) at 1 μg L^{-1} in the presence of DOM (with mid-DOC water) using an XPS-ESCALAB Xi+ Thermo Scientific instrument with an Al Kα radiation source. The binding energies of spectra were calibrated to a C 1s peak at 284.8 eV.

Analytical Measurements. Filtered aqueous samples were analyzed for THg by transferring the water samples into an acid-cleaned, 40 mL glass vial (Thermo Scientific), and the samples were digested overnight with an acidic mixture of potassium permanganate and potassium persulfate at 80 °C.[33] Filtered aqueous samples were analyzed for MeHg by preserving the samples with 0.4% trace-metal-grade hydrochloric acid (Fisher Scientific)[34] and kept in the dark at 4 °C before distillation. We also measured the solution pH at the end of the sorption and incubation trials using a daily-calibrated pH meter (Mettler Toledo) and DOC with a total organic carbon analyzer (Shimadzu).

All sediment samples were immediately frozen at −20 °C and subsequently lyophilized with a benchtop freeze-dryer (SP Scientific). The dry sediments were sieved through an acid-cleaned 1 mm polypropylene mesh to remove larger particles and measured THg and MeHg. Concentrations of Hg(II) in the sediments were calculated by subtracting measured MeHg from THg. To understand the effect of the sorbents on inorganic Hg and MeHg partitioning, sediment−water partition coefficients for both Hg(II) and MeHg ($\log K_{d,Hg(II)}$) were calculated as the sedimentary concentration in ng kg^{-1} divided by the aqueous concentration in ng L^{-1}.[13] Total amount of THg and MeHg as well as alteration of percentage of THg as MeHg (% MeHg) in each incubation microcosm were calculated to assess the Hg methylation potential of the sediment incubation experiment impacted by sorbent addition.[30,35] Detailed analytical procedures for THg and MeHg both water and sediment and quality assurance data can be found in Text S2.

https://doi.org/10.1021/acs.est.2c01591
Environ. Sci. Technol. 2022, 56, 11835−11844

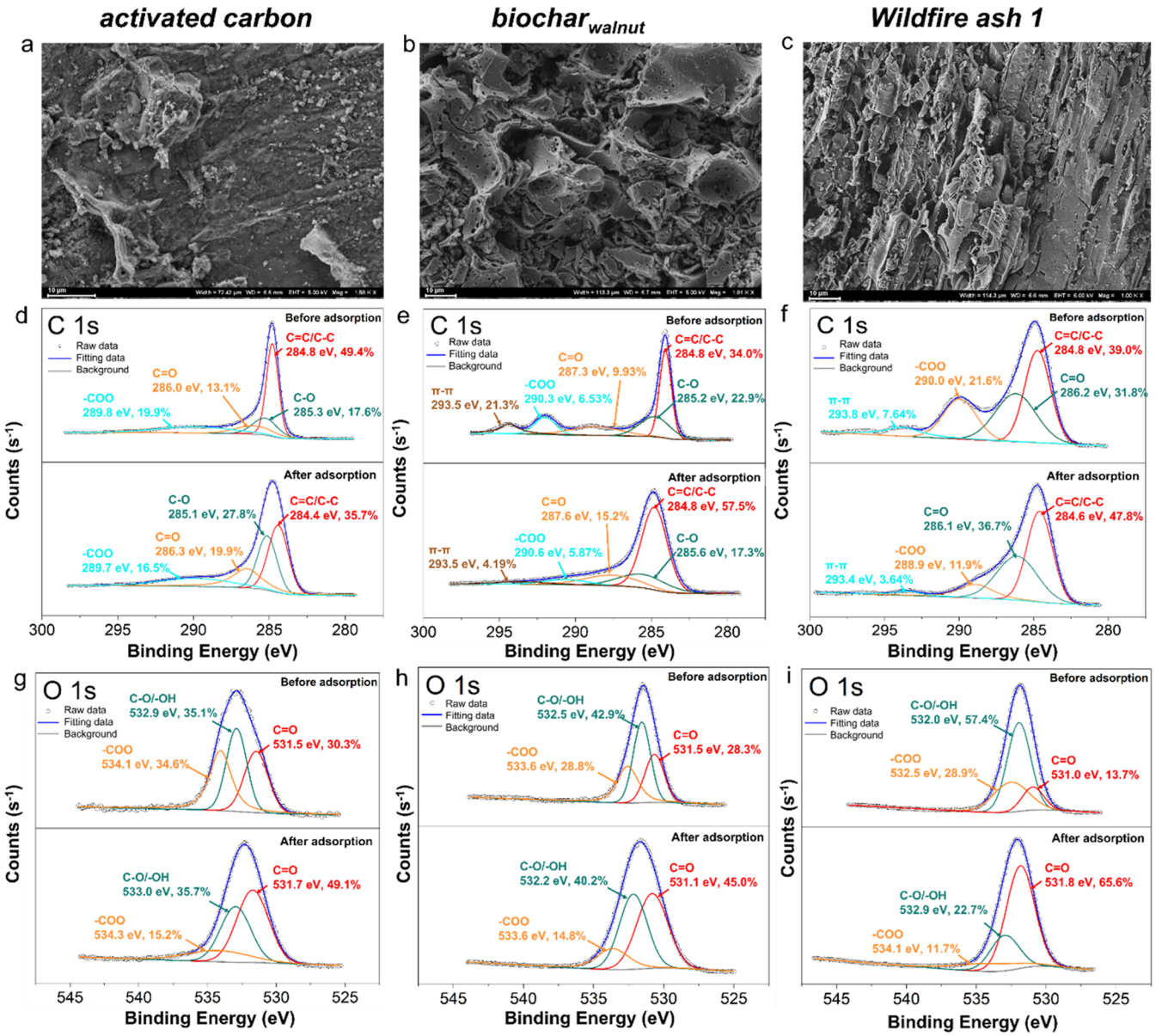

Figure 1. (a–c) SEM images of activated carbon, biochar$_{walnut}$, and wildfire ash 1. (d–f) High-resolution XPS spectra of C 1s for activated carbon, biochar$_{walnut}$, and wildfire ash 1 before and after reacting with Hg(II). (g–i) High-resolution XPS spectra of O 1s for activated carbon, biochar$_{walnut}$, and wildfire ash 1 before and after Hg reactions.

Statistical Analyses. Nonlinear regression analysis was performed using OriginPro 2021 (OriginLab Corporation, Northampton, MA) since the linearization might result in an inherent bias, diverse estimation errors, and fit distortions. Hence, nonlinear modeling is considered a more robust approach for estimating kinetic and isotherm parameters.[36] All linear regression analyses were performed using OriginPro 2021. One-way analysis of variance (ANOVA) with Student–Newman–Keulsa multiple comparison tests was performed using SigmaPlot 12.5 (Systat Software, Palo Alto, CA). The significance level for all statistical analyses was set at $p = 0.05$.

RESULTS AND DISCUSSION

Basic Sorbent Characteristics and Hg–Sorbent Interactions. There was a large range of C contents (10–71%) among the tested solid sorbents. Both activated carbon and biochars had >50% C contents, whereas laboratory-controlled burn ash had intermediate (13–43%) and wildfire ash the lowest (10–17%) C contents (Table S1). Notably, there was a large range of residual Hg contents (0.4–59.0 ng g^{-1}) in the solid sorbents, being much higher in both low-temperature laboratory-controlled burn and wildfire ashes than those of activated carbon and biochars (2.6–10.6 ng g^{-1}). However, the laboratory-controlled burn ash generated at a high temperature (550*ox* and 550*py*) had negligible residual Hg (<1 ng g^{-1}) (Table S1).

SEM micrographs of the three representative sorbents (activated carbon, biochar$_{walnut}$, and wildfire ash 1) indicated the prevalence of square morphologies and micropores with rough surfaces on activated carbon (Figure 1a). The biochar$_{walnut}$ micrograph showed the presence of many large pores and different morphologic irregularities on the surface (Figure 1b). The SEM micrograph of the wildfire ash 1 displayed a porous-folded structure (Figure 1c); such features

https://doi.org/10.1021/acs.est.2c01591
Environ. Sci. Technol. 2022, 56, 11835–11844

can contribute to increased surface area and an elevated reactivity in interfacial reactions of the ash samples,[37] potentially enhancing the aqueous sorption capability of Hg(II) by wildfire ash 1 (see results below).

XPS characterization of sorbent materials before and after reaction with aqueous Hg(II) displayed a clear Hg 4f peak for wildfire ash 1. In contrast, the Hg 4f peak for activated carbon and biochar$_{walnut}$ was not clear, possibly owing to the low Hg(II) level (1 μg L^{-1}) used in this evaluation (Figure S1). The high-resolution Hg 4f spectra for activated carbon, biochar$_{walnut}$, and wildfire ash 1 after Hg adsorption were fitted with a single Hg 4f spin−orbit split doublet (the Hg 4f$_{5/2}$ and Hg 4f$_{7/2}$ peaks).[19,38] The reasons for the absence of a spin−orbit for Hg 4f are unknown, but doublet peaks appeared at 101.6 and 102.6 eV for activated carbon, 101.6 and 102.1 eV for biochar$_{walnut}$, and 100.7 and 101.6 eV for wildfire ash 1 (Figure S1). The same peak at 101.6 eV revealed that Hg was adsorbed in a similar Hg form ((−COO)$_2$Hg) by activated carbon, biochar$_{walnut}$, and wildfire ash 1.

A shift of the binding energy for C 1s and O 1s was observed for activated carbon, biochar$_{walnut}$, and wildfire ash 1 before and after Hg adsorption (Figure 1d−i and Table S2), implying the involvement of C- and/or O-containing functional groups in Hg adsorption.[19,39] Strikingly, after Hg adsorption by activated carbon, biochar$_{walnut}$, and wildfire ash 1, the carboxylic (−COO) group in O 1s decreased from 35 to 15%, 29 to 15%, and 29 to 12%, respectively, and the decreasing trend was consistent with the findings from C 1s (Figure 1d−i and Table S2). The peak of Hg at 101.6 eV was assigned to complexes of (−COO)$_2$Hg (Figure S1).[19,40] These results confirm a similar Hg adsorption mechanism for activated carbon, biochar$_{walnut}$, and wildfire ash 1 that involves the formation of complexes between Hg and oxygen-containing functional groups, especially the −COO group.

Unlike biochar$_{walnut}$ and wildfire ash 1, Hg adsorption by activated carbon resulted in a decrease of C content in the C═C group by 14% (Figure 1d), suggesting that Hg removal by activated carbon was also attributed to the formation of Hg−Cπ bonds.[40] Previous studies demonstrated that delocalized lone-pair π electrons were associated with graphite-like domains of plant-derived biochars.[41,42] We found that the quantity of π−π groups in biochar$_{walnut}$ decreased substantially from 21 to 4.2% (Figure 1e), indicating that π electrons may be involved in the removal of Hg onto the biochar$_{walnut}$. However, electrostatic interactions seem unlikely to be involved when the dominant Hg species is uncharged Hg(OH)$_2$.[43] This suggests two possible alternative sorption mechanisms: (i) π electrons could be involved in the reduction of Hg(II) to Hg(I) on the C surfaces;[43,44] and/or (ii) Hg(II) might complex with C═C and C═O to form Hg-π binding between Hg and a graphite-like structure (C═C) and C═O in biochars.[19] Notably, the C content in the C═O group decreased by 6% in biochar$_{walnut}$ after Hg adsorption (Figure 1e). Like biochar$_{walnut}$, the peak of π−π bonds for wildfire ash 1 decreased from 8 to 4% after Hg adsorption, suggesting that π electrons may also be involved in Hg removal by wildfire ash 1.

Unlike activated carbon and biochar$_{walnut}$, the O content in the C−O/−OH group decreased by 35%, and the C═O group increased by 52% after Hg adsorption by wildfire ash 1 (Figure 1i). These shifts infer that phenolic hydroxyl groups might participate in the reduction of Hg(II) during Hg adsorption by wildfire ash 1, consistent with the adsorption mechanism proposed for bagasse biochar in which the reduction of Hg(II) by phenol was involved in Hg removal.[19] Thus, considering Hg(OH)$_2$ as the dominant Hg species in this work at pH > 7,[43] Hg adsorption to the contrasting sorbent materials is posited as: (i) carboxylic and graphite-like structures were the predominant binding sites for activated carbon; (ii) carboxylic and π electrons were the major binding sites for biochar$_{walnut}$; and (iii) carboxylic and phenolic hydroxyl groups were the primary binding sites for wildfire ash 1.

Aqueous Sorption of Hg(II). In the absence of added Hg(II), there were noticeable changes in DOC concentrations in the presence of activated carbon, biochar$_{walnut}$, biochar$_{sawdust}$, wildfire ash 1, and wildfire ash 2 for the different initial DOC levels (i.e., low-, mid-, and high-DOC) (Figure 2). Specifically,

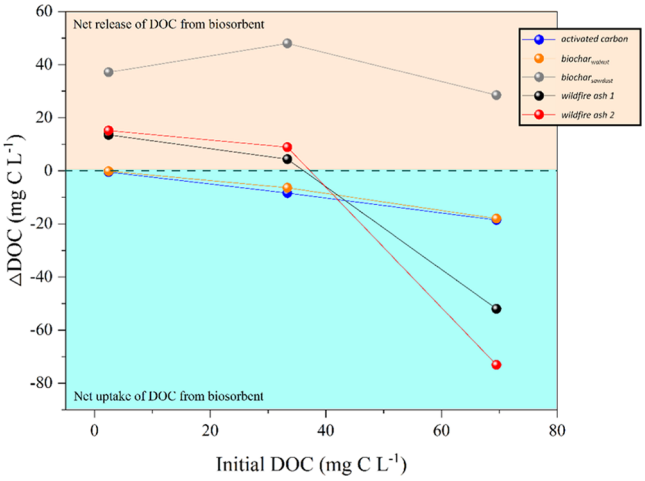

Figure 2. Change of DOC (ΔDOC) per unit mass of carbon in different solid sorbents (i.e., biosorbent stated in the graph) in water of different initial DOC levels (low-DOC: 2.4 mg C L^{-1}; mid-DOC: 33.4 mg C L^{-1}; high-DOC: 69.5 mg C L^{-1}) after 48 h.

in low-DOC water, all sorbents, except activated carbon and biochar$_{walnut}$, showed a net release of DOC. In mid-DOC water, the magnitude of net DOC uptake increased for activated carbon and biochar$_{walnut}$, whereas the net DOC release was reduced for wildfire ash 1 and wildfire ash 2. In high-DOC water, all sorbents, except biochar$_{sawdust}$, showed a strong net uptake of DOC from the solution (Figure 2). Only activated carbon and biochar$_{walnut}$ consistently retained DOC at all of the DOC levels tested. Such DOC-dependent properties for DOC release/uptake by the solid-phase sorbents are especially important for determining aqueous Hg(II) removal as DOM (through thiol groups) forms strong soluble Hg complexes in natural waters.[45]

Aqueous Hg(II) adsorption by activated carbon, two biochars (biochar$_{walnut}$ and biochar$_{sawdust}$), four laboratory-controlled burn ash (250*py*, 250*ox*, 550*py*, 550*ox*), and two wildfire ash (wildfire ash 1 and wildfire ash 2) samples are shown in Figure 3 and Table S3. Notably, both "natural" wildfire ash samples exhibited a similar equilibrium adsorption capacity (q_e) to activated carbon and biochar$_{walnut}$ in low-DOC water (Figure 3 and Table S3). Clearly, DOC had strong effects on the q_e of wildfire ash when compared to that of activated carbon and biochar$_{walnut}$ (Figure 3 and Table S3). Interestingly, both natural wildfire ash samples had significantly higher q_{ec} values (expressed as Hg sorbed per unit mass of C) (p < 0.05) than activated carbon and the two biochars tested

https://doi.org/10.1021/acs.est.2c01591
Environ. Sci. Technol. 2022, 56, 11835−11844

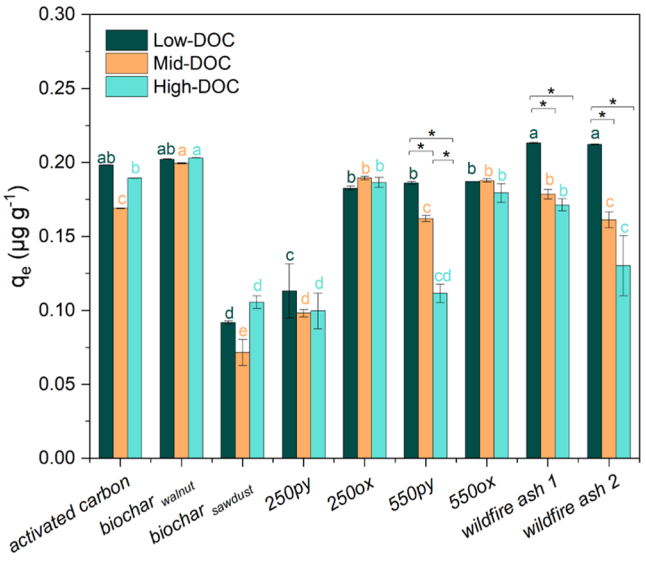

Figure 3. Adsorption capacity of Hg(II) by activated carbon, biochar$_{walnut}$, biochar$_{sawdust}$, lab-controlled-burn ash (250*py*, 250*ox*, 550*py*, and 550*ox*), wildfire ash 1, and wildfire ash 2 under different DOC level waters (low-DOC, mid-DOC, and high-DOC) spiked with 1 μg L^{-1} of Hg(II). The asterisk above the bars indicates a significant difference of the same adsorbents among different DOC water treatments (one-way ANOVA, * means $p < 0.05$, without * means $p > 0.05$), and the values that are statistically different ($p < 0.05$) among treatments with different solid sorbents under the same DOC level according to one-way ANOVA are indicated by lowercase letters. q_e indicates the equilibrium quantity of adsorbed Hg(II) on per unit mass of sorbent. Error bars represent standard deviation.

(Table S3), which may result from Hg(II) being bound by sorption or coprecipitation with mineral components, rather than exclusively with organic moieties (Table S1),[46,47] in addition to potential interactions with the black carbon fraction of the wildfire ash samples.[9]

For the laboratory-controlled burn ash, the material generated under oxidation conditions (0.18−0.19 μg g^{-1} at 250 and 550 °C) had significantly higher q_e values than ash produced under pyrolysis (0.10−0.11 μg g^{-1} at 250 °C and 0.11−0.18 μg g^{-1} at 550 °C) ($p < 0.05$) (Figure 3 and Table S3). The wildfire ash and laboratory-controlled burn ash displayed quite different q_e values, with wildfire ash 1 and wildfire ash 2 being significantly higher than those of 250*py* and 550*py* ash samples ($p < 0.05$) but similar to those of 250*ox* and 550*ox* ($p > 0.05$). Consistently, wildfire ash 1, wildfire ash 2, and 550*py* all showed a significant declining trend of q_e values with increasing DOC (Figure 3 and Table S3), indicating a competition between DOM and the solid-phase sorbents for aqueous Hg(II). This corroborates previous observations of a negative relationship between DOM concentration and sorbent removal of Hg(II).[22,23]

To further evaluate the q_e of activated carbon, two biochars, and two wildfire ash samples, sorption isotherms for Hg(II) were determined. The q_e of all sorbents linearly increased with increasing initial Hg(II) concentration (C_0) for all three DOC levels (Figure S3). The Langmuir model well described the sorption isotherms for all sorbents, except for a low r^2 value for biochar$_{sawdust}$ in high-DOC water (Table S4). The strong Langmuir model fit suggests that the adsorption process for Hg(II) by these sorbents proceeds as a monolayer adsorption phenomenon.[29] Notably, the theoretical adsorption capacity

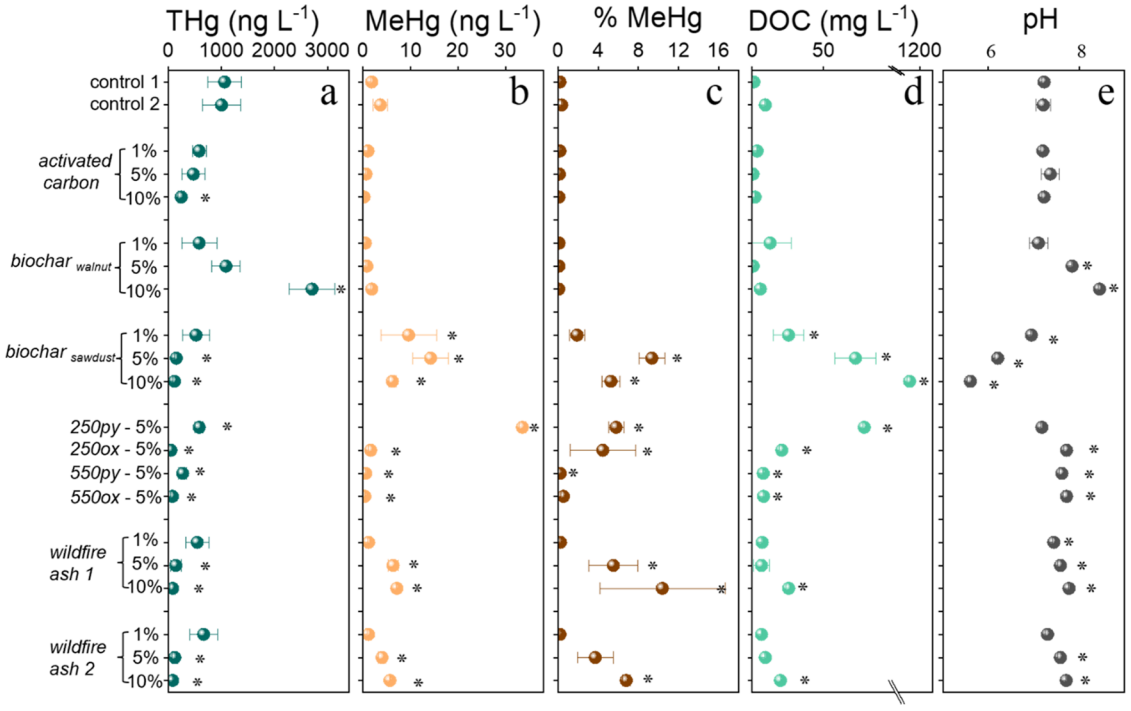

Figure 4. Effects of activated carbon, biochar$_{walnut}$, biochar$_{sawdust}$, lab-controlled burn ash (250*py*, 250*ox*, 550*py*, and 550*ox*), wildfire ash 1, and wildfire ash 2 on (a) filtered THg, (b) filtered MeHg, (c) % MeHg, (d) DOC, and (e) pH after 14 days of anoxic sediment incubation. The 1, 5, and 10% contents indicate the amendment level of solid sorbents with sediments. Two independent control samples (control 1 for activated carbon, biochar, and wildfire ash incubations and control 2 for lab-controlled burn ash incubations) were included. Each bars are standard deviation for triplicate samples. Asterisk indicates significantly different values from control based on one-way ANOVA ($p < 0.05$) and Student−Newman−Keuls comparisons.

https://doi.org/10.1021/acs.est.2c01591
Environ. Sci. Technol. 2022, 56, 11835−11844

(q_m) for Hg(II) on wildfire ash 1 (15.5 $\mu g\ g^{-1}$) and wildfire ash 2 (12.2 $\mu g\ g^{-1}$) in mid-DOC water was similar to that of activated carbon (13.9 $\mu g\ g^{-1}$), but much higher than for both biochar samples (<5 $\mu g\ g^{-1}$) (Table S4). These results clearly indicate the strong Hg(II) sorption characteristics by activated carbon and the wildfire ash materials even in the presence of natural DOM.

Finally, kinetic experiments demonstrated that 96% of Hg(II) was quickly removed in the first 0.5 h by biochar$_{walnut}$, whereas 94% of Hg(II) was removed by wildfire ash 1 and wildfire ash 2 in the first 4 hours. In contrast, only 91% of Hg(II) was removed by activated carbon after 12 h (Figure S3). In low-DOC water, >90% of Hg(II) was removed in the first 0.5 h by all materials except for biochar$_{sawdust}$ (Figure S3), but a longer time would be required to remove 90% of Hg(II) in higher DOC waters, revealing that the presence of ambient DOM slows Hg(II) sorption by biosorbents.[22,23] Meanwhile, when we carried out kinetic studies in high-DOC water, the Hg adsorption rate increased rapidly in the first 1 h for wildfire ash 1 and wildfire ash 2, but then decreased during the following hours before achieving an apparent equilibrium after 48 h (Figure S3). We ascribe the rapid initial rate of aqueous sorption during the first hour to the adsorption of labile Hg(II), whereas subsequent release of DOM from the sorbent resulted in competition and a slowing sorption process. Similarly, the net release of DOM from biochar$_{sawdust}$ (Figure 2) may be responsible for the lack of Hg(II) reaching equilibrium during the 48 h equilibration period. These findings further demonstrate the importance of DOM as a strong competing ligand for Hg(II) complexation with the binding sites on the solid-phase sorbents.

Effect of Solid Sorbents on Sedimentary Mercury Mobilization and Methylation. Relatively high levels of Hg(II) were mobilized from the Hg-contaminated South River sediments after 14 days of sealed incubation, with an average filtered THg concentration of 1,033 ng L^{-1}. The addition of solid-phase sorbents (1, 5, and 10% addition levels) reduced filtered THg concentrations to a range from 52 to 669 ng L^{-1}, with the exception of the 10% biochar$_{walnut}$ treatment in which filtered THg concentration strikingly increased to 2,710 ng L^{-1} (Figure 4 and Table S5). At the 5% addition level, the sorbents displayed the following order in reducing filtered THg during the 2 week anoxic incubation: 250ox ~ 550ox > wildfire ash 2 ~ wildfire ash 1 ~ biochar$_{sawdust}$ > activated carbon ~ 550py ~ 250py ≫ biochar$_{walnut}$. In general, as the sorbent addition level increased, the filtered THg concentrations decreased for activated carbon (by 45 and 77%; 5 and 10% addition relative to the control, respectively), biochar$_{sawdust}$ (by 37 and 92%), wildfire ash 1 (by 48 and 92%), and wildfire ash 2 (by 50 and 88%) (Figure 4 and Table S5). In contrast, increasing the addition level of biochar$_{walnut}$ resulted in even higher filtered THg concentrations (Figure 4) that we attribute, in part, to the increase of pH (from 7.1 to 8.5) with increasing biochar$_{walnut}$ levels as desorption of soil Hg(II) has been shown to increase with increasing pH values from 7 to 9.[48] In general, both biochar and wildfire ash materials can be alkaline (pH 9−12), with the pH values increasing as the production temperature increases.[49] We also observed a strong inverse, nonlinear relationship between (filtered) THg and DOC in the treatments with the two wildfire ash samples (Figure S4a), implying potential decoupling of DOM and Hg(II) in the dissolved phase under anoxic conditions.

Among laboratory-controlled burn ash samples, the 5% addition level of 250*ox* and 550*ox* reduced THg by 95 and 92% (compared to control), respectively, which were considerably more effective than the corresponding pyrolysis counterparts of 250*py* (by 42%) and 550*py* (by 73%) (Table S5). Notably, a significantly higher aromatic hydrocarbon content was detected in 250*ox* (45.0 ± 3.4%), 550*ox* (50.8 ± 3.7%), and 550*py* (52.0 ± 5.1%) than that in 250*py* (25.9 ± 3.9%) (data from Chen et al., in review), possibly implying a role for aromatic hydrocarbon compounds in reducing Hg(II) mobilization from the contaminated sediment. These findings corroborated the findings of Ku et al.[9] in which higher aromatic hydrocarbon content materials tended to limit Hg release to the aqueous phase. Moreover, the ash produced under oxidation conditions (i.e., in the presence of oxygen and a high temperature of 450−1,400 °C) was more effective in sequestering sedimentary Hg(II) than ash produced under pyrolysis conditions (i.e., under limited oxygen and a lower temperature from 250 to 450 °C).[25]

In contrast to the high Hg mobilization from sediments, the control treatment resulted in relatively low levels of filtered MeHg (1.8 and 3.7 ng L^{-1}), and the various solid-phase sorbent addition showed variable effectiveness in reducing (filtered) MeHg concentrations (Figure 4 and Table S5). The activated carbon and two of the laboratory-controlled burn ash samples (550*py* and 550*ox*) reduced MeHg levels in the incubated samples, whereas the other sorbents produced no effect or even slightly promoted MeHg concentrations in the aqueous phase. The stimulation of MeHg production seems contradictory to the ash-only incubation study by Ku et al.[9] in which the authors observed little Hg(II) and MeHg in the aqueous phase; we believe that the presence of a contaminated sediment in the current study would provide much more bioavailable Hg(II) and labile organic matter, and these conditions would be more stimulative to Hg(II) methylation than ash-only conditions. The higher aqueous MeHg concentrations may be associated with the higher DOC concentrations in wildfire ash 1 (r^2 = 0.622; p < 0.05) and wildfire ash 2 (r^2 = 0.707; p < 0.05) treatments (Figure S4b). Previous studies have demonstrated that DOC can be utilized by microbial Hg methylators as an electron donor to facilitate conversion of Hg(II) to MeHg.[50,51]

Possible reasons for such a low percentage of MeHg yield include the relatively low organic matter content (loss-on-ignition measured at 7%)[52] of the relatively coarse, contaminated sediments that may limit microbial activity, and also the very high background Hg levels in the sediment that resulted in only a small fractional conversion of THg to MeHg. Another potential reason would be the inhibition of MeHg production due to elevated THg sedimentary levels (13.4 $\mu g\ g^{-1}$) as a field study in the historic Hg mining area in Yolo County, California, observed decreasing MeHg with increasing THg in sediments above the THg level of 17 $\mu g\ g^{-1}$.[53]

Consistent with published data from another sorbent addition study,[13] bulk sediment THg concentrations were not a good predictor of the effectiveness of sorbents, but sedimentary MeHg concentrations in biochar$_{sawdust}$, wildfire ash 1, wildfire ash 2, and 250*py* additions were 42, 97, 85, and 103% higher than controls (Table S6). Previous studies have demonstrated that the increase in sedimentary MeHg with sorbent addition could have arisen from higher rates of gross MeHg production or reduced MeHg efflux to overlying

https://doi.org/10.1021/acs.est.2c01591
Environ. Sci. Technol. 2022, 56, 11835−11844

water.[13,23] Notably, the partition coefficients of MeHg ($\log K_d$ MeHg) in sediments with additions of biochar$_{sawdust}$, wildfire ash 1, wildfire ash 2, and 250*py* were not significantly different from the control treatment ($p > 0.05$) (Figure S5). However, with higher $\log K_d$ of Hg(II) (Figure S5) and whole microcosm percentage of MeHg (i.e., both water and sediment) (Figure S6) being observed in treatments with biochar$_{sawdust}$, wildfire ash 1, wildfire ash 2, and 250*py*, the results may imply that these sorbents may disproportionately increase the availability of Hg(II) for microbial Hg methylators and may result in higher Hg(II) methylation yields under evelated DOC conditions.[54,55] Direct study of DOM characteristics and microbial Hg(II) methylation[56] of these incubation samples will be needed to better understand the complex biogeochemical processes.

It is worth noting that Hg methylation trends in the present study were limited to a relatively short term (2 weeks). Despite the strong sorption toward Hg(II) by wildfire ash, which contributes to the inhibition of MeHg production, on the other hand, the nutrients released by ash[4] may aid in promoting microbial MeHg production as indicated by the MeHg data, and perhaps MeHg can be degraded in the longer term.[54] Therefore, the ecological risk of wildfire to the downstream water environment in the long term is still entirely unclear and needs further investigation.

Environmental Implications. This work demonstrates that ash produced by wildfire and prescribed burning has a significant impact on aquatic Hg cycling processes by sequestering aqueous Hg, mediating sedimentary Hg mobilization, and altering its conversion to highly toxic MeHg. Wildfire ash materials are readily transported to aquatic systems through runoff/erosion and hydrologic transport following wildfires.[24] Per unit mass of bulk or C content, we found that wildfire ash had the highest sorption capabilities for aqueous Hg(II), as compared to activated carbon and selected biochars. The Hg adsorption mechanisms appear to differ among the sorbents evaluated: (i) carboxylic and graphite-like structures were the predominant binding sites for activated carbon; (ii) carboxylic and π electrons were the major binding sites for biochar$_{walnut}$; and (iii) carboxylic and phenolic hydroxyl groups were the primary binding sites for wildfire ash. DOM leaching from some sorbent materials reduced their net Hg sequestration effectiveness owing to competition for aqueous Hg(II) between the solid-phase sorbents and aqueous-phase DOM.

While the effectiveness of activated carbon for inhibiting MeHg production and bioaccumulation in Hg-contaminated aquatic ecosystems has been previously demonstrated,[13,14] we also confirmed that certain biochars, laboratory-controlled burn ash, and wildfire ash materials altered aqueous Hg(II) levels, bioavailability of Hg(II), and sedimentary Hg methylation. Nevertheless, while wildfire ash can strongly sequester aqueous Hg(II), leaching of its labile organic matter may mobilize sedimentary Hg(II) and/or promote the production of toxic MeHg that can bioaccumulate/biomagnify in downstream aquatic habitats. A similar observation on increased MeHg bioaccumulation was reported in a downstream lake in Alberta, Canada, after wildfire, partly due to restructuring of food web structure in the lake.[57] These findings indicate that wildfire ash, especially those generated under low-intensity wildfire (i.e., resulting in black ash), can have appreciable effects on Hg cycling processes in aquatic ecosystems (rivers, wetlands, reservoirs, lakes) and should be considered in post-fire aquatic ecosystem restoration activities and also within the context of the global Hg cycle.[58] In addition to the increasing adoption of prescribed burning, wildfire impacts on aquatic Hg cycling are expected to greatly increase as the number, size, and intensity of wildfires rapidly increase with climate change.

■ ASSOCIATED CONTENT

Supporting Information

The Supporting Information is available free of charge at https://pubs.acs.org/doi/10.1021/acs.est.2c01591.

Tabulated information on the physical and chemical properties of the solid sorbents, spectroscopic characterization of the sorbent surfaces before and after sorption with aqueous Hg(II), equilibrium quantity of adsorbed Hg(II) in aqueous sorption tests, isotherm model parameters for Hg(II), and sealed sediment incubation data; graphical illustration of XPS spectra, equilibrium adsorption capacity of Hg(II) at different initial Hg(II) concentrations, effect of contact time on Hg(II) adsorption, and relationships between DOC and Hg(II) or MeHg after 2 weeks of sediment incubation (PDF)

■ AUTHOR INFORMATION

Corresponding Authors

Martin Tsz-Ki Tsui − *Department of Biology, University of North Carolina at Greensboro, Greensboro, North Carolina 27402, United States; School of Life Sciences, State Key Laboratory of Agrobiotechnology, The Chinese University of Hong Kong, Shatin, NT, Hong Kong SAR, China;* orcid.org/0000-0003-2002-1530; Phone: +852-39436123; Email: mtktsui@cuhk.edu.hk; Fax: +852-26037246

Zhang Cheng − *College of Environmental Science, Sichuan Agricultural University, Chengdu 611130, China;* orcid.org/0000-0001-6211-3017; Email: cz@sicau.edu.cn

Xue-Mei Zhu − *College of Environmental Science, Sichuan Agricultural University, Chengdu 611130, China;* Email: zhuxuemei@sicau.edu.cn

Authors

Han-Han Li − *College of Environmental Science, Sichuan Agricultural University, Chengdu 611130, China; Department of Biology, University of North Carolina at Greensboro, Greensboro, North Carolina 27402, United States*

Peijia Ku − *Department of Biology, University of North Carolina at Greensboro, Greensboro, North Carolina 27402, United States; Environmental Sciences Division, Oak Ridge National Laboratory, Oak Ridge, Tennessee 37831, United States;* orcid.org/0000-0003-2813-9269

Huan Chen − *Biogeochemistry & Environmental Quality Research Group, Clemson University, Georgetown, South Carolina 29442, United States;* orcid.org/0000-0001-9998-1205

Ziyu Yin − *Department of Nanoscience, Joint School of Nanoscience and Nanoengineering, University of North Carolina at Greensboro, Greensboro, North Carolina 27401, United States*

Randy A. Dahlgren − *Department of Land, Air and Water Resources, University of California, Davis, California 95616, United States*
Sanjai J. Parikh − *Department of Land, Air and Water Resources, University of California, Davis, California 95616, United States*
Jianjun Wei − *Department of Nanoscience, Joint School of Nanoscience and Nanoengineering, University of North Carolina at Greensboro, Greensboro, North Carolina 27401, United States;* orcid.org/0000-0002-2658-0248
Tham C. Hoang − *School of Fisheries, Aquaculture, and Aquatic Sciences, Auburn University, Auburn, Alabama 36849, United States*
Alex T. Chow − *Biogeochemistry & Environmental Quality Research Group, Clemson University, Georgetown, South Carolina 29442, United States;* orcid.org/0000-0001-7441-8934

Complete contact information is available at: https://pubs.acs.org/10.1021/acs.est.2c01591

Notes

The authors declare no competing financial interest.

■ ACKNOWLEDGMENTS

The authors acknowledge the funding support by the China Scholarship Council to H.L. for undertaking this overseas exchange program. This study was financially supported by the National Science Foundation awards (EAR-1711642 and CBET-1917156) and the National Institute of Food and Agriculture award (2018-67019-27795) both to M.T.-K.T. and A.T.C.

■ REFERENCES

(1) Scharenbroch, B. C.; Nix, B.; Jacobs, K. A.; Bowles, M. L. Two decades of low-severity prescribed fire increases soil nutrient availability in a Midwestern, USA oak (Quercus) forest. *Geoderma* **2012**, *183*−*184*, 80−91.
(2) Westerling, A. L.; Hidalgo, H. G.; Cayan, D. R.; Swetnam, T. W. Warming and earlier spring increase western US forest wildfire activity. *Science* **2006**, *313*, 940−943.
(3) Francos, M.; Úbeda, X. Prescribed fire management. *Curr. Opin. Environ. Sci. Health* **2021**, *21*, No. 100250.
(4) Rhoades, C. C.; Chow, A. T.; Covino, T. P.; Fegel, T. S.; Pierson, D. N.; Rhea, A. E. The legacy of a severe wildfire on stream nitrogen and carbon in headwater catchments. *Ecosystems* **2019**, *22*, 643−657.
(5) Fitzgerald, W. F.; Engstrom, D. R.; Mason, R. P.; Nater, E. A. The case for atmospheric mercury contamination in remote areas. *Environ. Sci. Technol.* **1998**, *32*, 1−7.
(6) St Louis, V. L.; Rudd, J. W. M.; Kelly, C. A.; Hall, B. D.; Rolfhus, K. R.; Scott, K. J.; Lindberg, S. E.; Dong, W. Importance of the forest canopy to fluxes of methyl mercury and total mercury to boreal ecosystems. *Environ. Sci. Technol.* **2001**, *35*, 3089−3098.
(7) Webster, J. P.; Kane, T. J.; Obrist, D.; Ryan, J. N.; Aiken, G. R. Estimating mercury emissions resulting from wildfire in forests of the Western United States. *Sci. Total Environ.* **2016**, *568*, 578−586.
(8) Tuhý, M.; Rohovec, J.; Matoušková, S.; Mihaljevič, M.; Kříbek, B.; Vaněk, A.; Mapani, B.; Göttlicher, J.; Steininger, R.; Majzlan, J.; Ettler, V. The potential wildfire effects on mercury remobilization from topsoils and biomass in a smelter-polluted semi-arid area. *Chemosphere* **2020**, *247*, No. 125972.
(9) Ku, P.; Tsui, M. T. K.; Nie, X.; Chen, H.; Hoang, T. C.; Blum, J. D.; Dahlgren, R. A.; Chow, A. T. Origin, reactivity, and bioavailability of mercury in wildfire ash. *Environ. Sci. Technol.* **2018**, *52*, 14149−14157.
(10) Regnell, O.; Watras, C. J. Microbial mercury methylation in aquatic environments: A critical review of published field and laboratory studies. *Environ. Sci. Technol.* **2019**, *53*, 4−19.
(11) Lavoie, R. A.; Jardine, T. D.; Chumchal, M. M.; Kidd, K. A.; Campbell, L. M. Biomagnification of mercury in aquatic food webs: A worldwide meta-analysis. *Environ. Sci. Technol.* **2013**, *47*, 13385−13394.
(12) Huang, C. P.; Blankenship, D. W. The removal of mercury(II) from dilute aqueous solution by activated carbon. *Water Res.* **1984**, *18*, 37−46.
(13) Gilmour, C. C.; Riedel, G. S.; Riedel, G.; Kwon, S.; Landis, R.; Brown, S. S.; Menzie, C. A.; Ghosh, U. Activated carbon mitigates mercury and methylmercury bioavailability in contaminated sediments. *Environ. Sci. Technol.* **2013**, *47*, 13001−13010.
(14) Gilmour, C.; Bell, T.; Soren, A.; Riedel, G.; Riedel, G.; Kopec, D.; Bodaly, D.; Ghosh, U. Activated carbon thin-layer placement as an *in situ* mercury remediation tool in a Penobscot River salt marsh. *Sci. Total Environ.* **2018**, *621*, 839−848.
(15) Ranganathan, K. Adsorption of Hg(II) ions from aqueous chloride solutions using powdered activated carbons. *Carbon* **2003**, *41*, 1087−1092.
(16) Zabihi, M.; Ahmadpour, A.; Asl, A. H. Removal of mercury from water by carbonaceous sorbents derived from walnut shell. *J. Hazard. Mater.* **2009**, *167*, 230−236.
(17) Gomez-Eyles, J. L.; Yupanqui, C.; Beckingham, B.; Riedel, G.; Gilmour, C.; Ghosh, U. Evaluation of biochars and activated carbons for in situ remediation of sediments impacted with organics, mercury, and methylmercury. *Environ. Sci. Technol.* **2013**, *47*, 13721−13729.
(18) Boutsika, L. G.; Karapanagioti, H. K.; Manariotis, I. D. Aqueous mercury sorption by biochar from malt spent rootlets. *Water Air Soil Pollut.* **2014**, *225*, 1−10.
(19) Xu, X.; Schierz, A.; Xu, N.; Cao, X. Comparison of the characteristics and mechanisms of Hg(II) sorption by biochars and activated carbon. *J. Colloid Interface Sci.* **2016**, *463*, 55−60.
(20) Wang, A. O.; Ptacek, C. J.; Blowes, D. W.; Gibson, B. D.; Landis, R. C.; Dyer, J. A.; Ma, J. Application of hardwood biochar as a reactive capping mat to stabilize mercury derived from contaminated floodplain soil and riveRWAnk sediments. *Sci. Total Environ.* **2019**, *652*, 549−561.
(21) Wang, Y.; Sun, Y.; He, T.; Deng, H.; Wang, Z.; Wang, J.; Zheng, X.; Zhou, L.; Zhong, H. Biochar amendment mitigates the health risks of dietary methylmercury exposure from rice consumption in mercury-contaminated areas. *Environ. Pollut.* **2020**, *267*, No. 115547.
(22) Johs, A.; Eller, V. A.; Mehlhorn, T. L.; Brooks, S. C.; Harper, D. P.; Mayes, M. A.; Pierce, E. M.; Peterson, M. J. Dissolved organic matter reduces the effectiveness of sorbents for mercury removal. *Sci. Total Environ.* **2019**, *690*, 410−416.
(23) Schwartz, G. E.; Sanders, J. P.; McBurney, A. M.; Brown, S. S.; Ghosh, U.; Gilmour, C. C. Impact of dissolved organic matter on mercury and methylmercury sorption to activated carbon in soils: Implications for remediation. *Environ. Sci.: Processes Impacts* **2019**, *21*, 485−496.
(24) Uzun, H.; Dahlgren, R. A.; Olivares, C.; Erdem, C. U.; Karanfil, T.; Chow, A. T. Two years of post-wildfire impacts on dissolved organic matter, nitrogen, and precursors of disinfection by-products in California stream waters. *Water Res.* **2020**, *181*, No. 115891.
(25) Bodí, M. B.; Martin, D. A.; Balfour, V. N.; Santín, C.; Doerr, S. H.; Pereira, P.; Cerdà, A.; Mataix-Solera, J. Wildland fire ash: Production, composition and eco-hydro-geomorphic effects. *Earth-Sci. Rev.* **2014**, *130*, 103−127.
(26) Wang, J. J.; Dahlgren, R. A.; Chow, A. T. Controlled burning of forest detritus altering spectroscopic characteristics and chlorine reactivity of dissolved organic matter: Effects of temperature and oxygen availability. *Environ. Sci. Technol.* **2015**, *49*, 14019−14027.
(27) Mukome, F. N. D.; Zhang, X.; Silva, L. C.; Six, J.; Parikh, S. J. Use of chemical and physical characteristics to investigate trends in biochar feedstocks. *J. Agric. Food Chem.* **2013**, *61*, 2196−2204.

(28) USEPA. *Methods for Measuring the Acute Toxicity of Effluents and Receiving Waters to Freshwater and Marine Organisms*; US Environmental Protection Agency: Washington, DC, USA, 2002.
(29) Fang, R.; Lu, C.; Zhong, Y.; Xiao, Z.; Liang, C.; Huang, H.; Gan, Y.; Zhang, J.; Pan, G.; Xia, X.; Xia, Y.; Zhang, W. Puffed rice carbon with coupled sulfur and metal iron for high-efficiency mercury removal in aqueous solution. *Environ. Sci. Technol.* **2020**, *54*, 2539−2547.
(30) Tsui, M. T. K.; Finlay, J. C.; Nater, E. A. Effects of stream water chemistry and tree species on release and methylation of mercury during litter decomposition. *Environ. Sci. Technol.* **2008**, *42*, 8692−8697.
(31) Chow, E.; Tsui, M. T. K. Elucidating microbial pathways of mercury methylation during litter decomposition. *Bull. Environ. Contam. Toxicol.* **2019**, *103*, 617−622.
(32) Washburn, S. J.; Blum, J. D.; Demers, J. D.; Kurz, A. Y.; Landis, R. C. Isotopic characterization of mercury downstream of historic industrial contamination in the South River, Virginia. *Environ. Sci. Technol.* **2017**, *51*, 10965−10973.
(33) Woerndle, G. E.; Tsui, M. T. K.; Sebestyen, S. D.; Blum, J. D.; Nie, X.; Kolka, R. K. New insights on ecosystem mercury cycling revealed by stable isotopes of mercury in water flowing from a headwater peatland catchment. *Environ. Sci. Technol.* **2018**, *52*, 1854−1861.
(34) Parker, J. L.; Bloom, N. S. Preservation and storage techniques for low-level aqueous mercury speciation. *Sci. Total Environ.* **2005**, *337*, 253−263.
(35) Mitchell, C. P. J.; Branfireun, B. A.; Kolka, R. K. Spatial characteristics of net methylmercury production hot spots in peatlands. *Environ. Sci. Technol.* **2008**, *42*, 1010−1016.
(36) Khan, T. A.; Khan, E. A.; Shahjahan. Removal of basic dyes from aqueous solution by adsorption onto binary iron-manganese oxide coated kaolinite: Non-linear isotherm and kinetics modeling. *Appl. Clay Sci.* **2015**, *107*, 70−77.
(37) Cerrato, J. M.; Blake, J. M.; Hirani, C.; Clark, A. L.; Ali, A. M.; Artyushkova, K.; Peterson, E.; Bixby, R. J. Wildfires and water chemistry: Effect of metals associated with wood ash. *Environ. Sci.: Processes Impacts* **2016**, *18*, 1078−1089.
(38) Wang, J.; Deng, B.; Chen, H.; Wang, X.; Zheng, J. Removal of aqueous Hg(II) by polyaniline: Sorption characteristics and mechanisms. *Environ. Sci. Technol.* **2009**, *43*, 5223−5228.
(39) Guo, X.; Li, M.; Liu, A.; Jiang, M.; Niu, X.; Liu, X. Adsorption mechanisms and characteristics of Hg^{2+} removal by different fractions of biochar. *Water* **2020**, *12*, No. 2105.
(40) Dong, X.; Ma, L. Q.; Zhu, Y.; Li, Y.; Gu, B. Mechanistic investigation of mercury sorption by Brazilian pepper biochars of different pyrolytic temperatures based on X-ray photoelectron spectroscopy and flow calorimetry. *Environ. Sci. Technol.* **2013**, *47*, 12156−12164.
(41) Bourke, J.; Manley-Harris, M.; Fushimi, C.; Dowaki, K.; Nunoura, T.; Antal, M. J. Do all carbonized charcoals have the same chemical structure? 2. A model of the chemical structure of carbonized charcoal. *Ind. Eng. Chem. Res.* **2007**, *46*, 5954−5967.
(42) Harvey, O. R.; Herbert, B. E.; Rhue, R. D.; Kuo, L. J. Metal interactions at the biochar-water interface: Energetics and structure-sorption relationships elucidated by flow adsorption microcalorimetry. *Environ. Sci. Technol.* **2011**, *45*, 5550−5556.
(43) Sánchez-Polo, M.; Rivera-Utrilla, J. Adsorbent−adsoRWAte interactions in the adsorption of Cd(II) and Hg(II) on ozonized activated carbons. *Environ. Sci. Technol.* **2002**, *36*, 3850−3854.
(44) Zhu, J.; Deng, B.; Yang, J.; Gang, D. Modifying activated carbon with hybrid ligands for enhancing aqueous mercury removal. *Carbon* **2009**, *47*, 2014−2025.
(45) Ravichandran, M. Interactions between mercury and dissolved organic matter—A review. *Chemosphere* **2004**, *55*, 319−331.
(46) El-Shafey, E. I. Removal of Zn(II) and Hg(II) from aqueous solution on a carbonaceous sorbent chemically prepared from rice husk. *J. Hazard. Mater.* **2010**, *175*, 319−327.
(47) Kong, H.; He, J.; Gao, Y.; Wu, H.; Zhu, X. Cosorption of phenanthrene and mercury(II) from aqueous solution by soybean stalk-based biochar. *J. Agric. Food Chem.* **2011**, *59*, 12116−12123.
(48) Jing, Y. D.; He, Z. L.; Yang, X. E. Effects of pH, organic acids, and competitive cations on mercury desorption in soils. *Chemosphere* **2007**, *69*, 1662−1669.
(49) Certini, G. Effects of fire on properties of forest soils: A review. *Oecologia* **2005**, *143*, 1−10.
(50) Chiasson-Gould, S. A.; Blais, J. M.; Poulain, A. J. Dissolved organic matter kinetically controls mercury bioavailability to bacteria. *Environ. Sci. Technol.* **2014**, *48*, 3153−3161.
(51) Liu, P.; Ptacek, C. J.; Blowes, D. W. Mercury complexation with dissolved organic matter released from thirty-six types of biochar. *Bull. Environ. Contam. Toxicol.* **2019**, *103*, 175−180.
(52) Ku, P.; Tsui, M. T. K.; Liu, S.; Corson, K. B.; Williams, A. S.; Monteverde, M. R.; Woerndle, G. E.; Hershey, A. E.; Rublee, P. A. Examination of mercury contamination from a recent coal ash spill into the Dan River, North Carolina, United States. *Ecotoxicol. Environ. Saf.* **2021**, *208*, No. 111469.
(53) Holloway, J. M.; Goldhaber, M. B.; Scow, K. M.; Drenovsky, R. E. Spatial and seasonal variations in mercury methylation and microbial community structure in a historic mercury mining area, Yolo County, California. *Chem. Geol.* **2009**, *267*, 85−95.
(54) Marvin-DiPasquale, M. C.; Oremland, R. S. Bacterial methylmercury degradation in Florida Everglades peat sediment. *Environ. Sci. Technol.* **1998**, *32*, 2556−2563.
(55) Ullrich, S. M.; Tanton, T. W.; Abdrashitov, S. A. Mercury in the aquatic environment: A review of factors affecting methylation. *Crit. Rev. Environ. Sci. Technol.* **2001**, *31*, 241−293.
(56) Mangal, V.; Stenzler, B. R.; Poulain, A. J.; Guéguen, C. Aerobic and anaerobic bacterial mercury uptake is driven by algal organic matter composition and molecular weight. *Environ. Sci. Technol.* **2019**, *53*, 157−165.
(57) Kelly, E. N.; Schindler, D. W.; St Louis, V. L.; Donald, D. B.; Vladicka, K. E. Forest fire increases mercury accumulation by fishes via food web restructuring and increased mercury inputs. *Proc. Natl. Acad. Sci. U.S.A.* **2006**, *103*, 19380−19385.
(58) Selin, N. E. Global change and mercury cycling: challenges for implementing a global mercury treaty. *Environ. Toxicol. Chem.* **2014**, *33*, 1202−1210.

https://doi.org/10.1021/acs.est.2c01591
Environ. Sci. Technol. 2022, 56, 11835−11844